water

MDPI

Article

Response of Low Flows of Polish Rivers to Climate Change in 1987–1989

Dariusz Wrzesiński [1], Andrzej A. Marsz [2], Leszek Sobkowiak [1,*] and Anna Styszyńska [2]

[1] Department of Hydrology and Water Management, Faculty of Geographical and Geological Sciences, Adam Mickiewicz University, Bogumiła Krygowskiego str. 10, 61-680 Poznań, Poland
[2] Association of Polish Climatologists, Krakowskie Przedmieście str. 30, 00-927 Warsaw, Poland
* Correspondence: lesob@amu.edu.pl

Abstract: The paper discusses changes in the low-flow regime of rivers in Poland, resulting from climate change that occurred between 1987 and 1989. The low-flow variability of rivers was measured with the use of the number of days with low flows (ND_{LF}) below a threshold value, which was adopted as the 0.1 (10%) percentile (Q_{10}) from the set of daily flows recorded in the multi-annual period 1951–2020 at 140 water gauges on 83 rivers. The analysis of the course of climate change over Poland showed that it was caused by macro-circulation conditions, controlled by changes in the intensity of thermohaline circulation in the North Atlantic (NA THC). Climate change consisted of a sharp increase in sunshine duration and air temperature, and a decrease in relative humidity after 1988. Along with the lack of changes in precipitation totals, characterized by a strong yearly variability, and an increase in field evaporation, it led to noticeable changes in the water balance. As a result, in 1989–2020, there was a significant increase in ND_{FL} detected in about 2/3 of the area of Poland. With the change in the NA THC phase and the macro-circulation conditions, there was also a change in the spatial distribution of areas drained by rivers with increased ND_{FL}. In 1951–1988, these included the eastern parts of Poland, while after the climate change (1989–2020), its western and south-western parts.

Keywords: rapid climate shift; river low flows; cause of warming up; thermohaline circulation; water balance; Poland; North Atlantic

check for updates

Citation: Wrzesiński, D.; Marsz, A.A.; Sobkowiak, L.; Styszyńska, A. Response of Low Flows of Polish Rivers to Climate Change in 1987–1989. *Water* **2022**, *14*, 2780. https://doi.org/10.3390/w14182780

Academic Editors: Xander Wang and Lirong Liu

Received: 25 June 2022
Accepted: 5 September 2022
Published: 7 September 2022

1. Introduction

Between 1987 and 1989, the macro-circulation conditions in the Atlantic-European circulation sector changed, which led to climate change over Europe. In Poland, this change was most clearly marked by an abrupt increase in sunshine duration and air temperature, as well as a change in the cloud structure and a decrease in relative humidity. Moreover, the structure of the winter NAO index changed toward an increase in the frequency of positive index values, and the annual geopotential increased significantly over Poland. The annual precipitation totals remained unchanged, within the range of their current, significant inter-annual variability.

An increase in air temperature and sunshine duration, and a decrease in relative humidity are factors influencing an increase in field evaporation (e.g., [1–3]), which should be reflected in shaping the water balance change. In turn, the water balance change should be reflected in the change in river flow regime, which particularly clearly manifested in an increase in the frequency of occurrence of low flows.

Correlations analyses with indices quantifying large-scale climate variability have been performed by many authors. For the European region, the most relevant modes of climate variability appear to be the North Atlantic Oscillation (NAO) and the Atlantic Multidecadal Oscillation (AMO) [4].

Shorthouse and Arnell [5] confirmed that during winter positive NAO phases, winter stream flows were generally higher in Northern Europe, and lower in Southern Europe,

while the authors of [6] proved that hydrological regimes most sensitive to NAO variations were located at the Northern and Southern extremities of Europe, i.e., in the Scandinavian and in the Iberian peninsulas. A few other studies focused on specific European regions, such as the British Islands [7,8] and Scandinavia [9]. On a country scale, the authors of [10] determined that a negative phase of winter NAO was generally followed by a negative anomaly of fall stream flows in England and Wales, while the authors of [11] concluded that positive phases of winter NAO were usually associated with pronounced summer droughts in Romania. Giuntoli et al. [4] analyzed low flows in France in relation to large scale climate indices and found that seasonal climate indices had stronger links with low-flow indices than their annual counterparts.

Until now, various studies on the hydrology of droughts and low flows on rivers in Poland paid little attention to the existing climate change, treating the hydrological conditions prevailing after 1951 as stationary, and the interest in the frequency or percentage of low flows during the year resulted to a greater extent from treating them rather as a measure of the occurrence of hydrological drought [12–19]. Szwed et al. [20] studied the effects of climate change on agriculture, water resources, and human health sectors in Poland, and the authors of [21] applied three drought indices: the Standardized Precipitation Index (SPI), Standardized Precipitation Evapotranspiration Index (SPEI), and Standardized Runoff Index (SRI), and the hydro-climatic data to hydro-meteorological drought projections into the 21st century for selected Polish catchments.

Therefore, the problem is whether the occurring climate changes have an impact on the water balance in Poland, and to what extent these changes in the water balance have an impact on the flow regime in Polish rivers.

The aim of this paper is to present the results of research on the change in the frequency of occurrence of low flows in Poland in the multi-annual period 1951–2020 divided into two sub-periods, treated as different phases of the climate change: In 1951–1988 preceding climate change, and in 1989–2020 following that change. The research focuses on two aspects of this variability, i.e., the variability that occurred as a function of time, and the changes in the number of days with low flows that occurred in space. The hydrological part of the study is preceded by a short discussion on the most important manifestations of changes in selected elements of climate, important in terms of shaping the water balance, and changes in the water balance that occurred in Poland as a result of climate change that took place in 1987–1989.

2. Materials

The hydro-meteorological data were obtained from the database of the Institute of Meteorology and Water Management–National Research Institute (IMGW-PIB) in Warsaw [22]. The analysis is based on the series of annual air temperature (T), annual precipitation totals (P), annual values of general cloudiness (N, 1/8), and annual values of relative humidity (f, %). In this study, the authors used the values of the above-mentioned climatic elements, which constituted the area averages of 28 stations that were relatively evenly distributed in Poland (Figure 1) and covered the multi-annual period 1951–2020. In order to indicate that these values were the area averages, they were respectively marked as T_{PL}, P_{PL}, N_{PL}, and f_{PL} in this paper.

The number of days with low flows (ND_{LF}) per year on Polish rivers was calculated based on the publicly available data of daily flows recorded at 140 water gauges on 83 Polish rivers in the multi-annual period 1951–2020 [22]. The geographical position of the analyzed water gauges is presented in Figure 1 and basic hydrological data on the studied rivers are shown in Table A1.

The number of annual sunshine duration (marked as SD_{PL}) was the average of five stations: Gdynia, Łódź, Kraków, Wrocław, and Puławy (Figure 1), and covered the period 1951–2018. Data from the Wrocław station were the combined sequences of the sunshine duration observations from the stations of the University of Wrocław (station Biskupin) and the University of Life Sciences in Wrocław (station Swojec). The combination of the

two ranks and their homogenization was carried out by the authors of [23]. The data from Kraków station were the continuous, fully homogeneous observatory series from the IGiGP observatory of the Jagiellonian University [24,25]. The series from Łódź station combined the data published from 1951–2000 by the authors of [26] with the data from IMGW-PIB (2001–2018). The data from Puławy station were derived from the IUNG observatory in Puławy, while the data from Gdynia were obtained from the IMGW-PIB station. The limited series of annual sunshine duration used to calculate the area average was justified by the fact that the sunshine duration data provided by IMGW-PIB started from 1966.

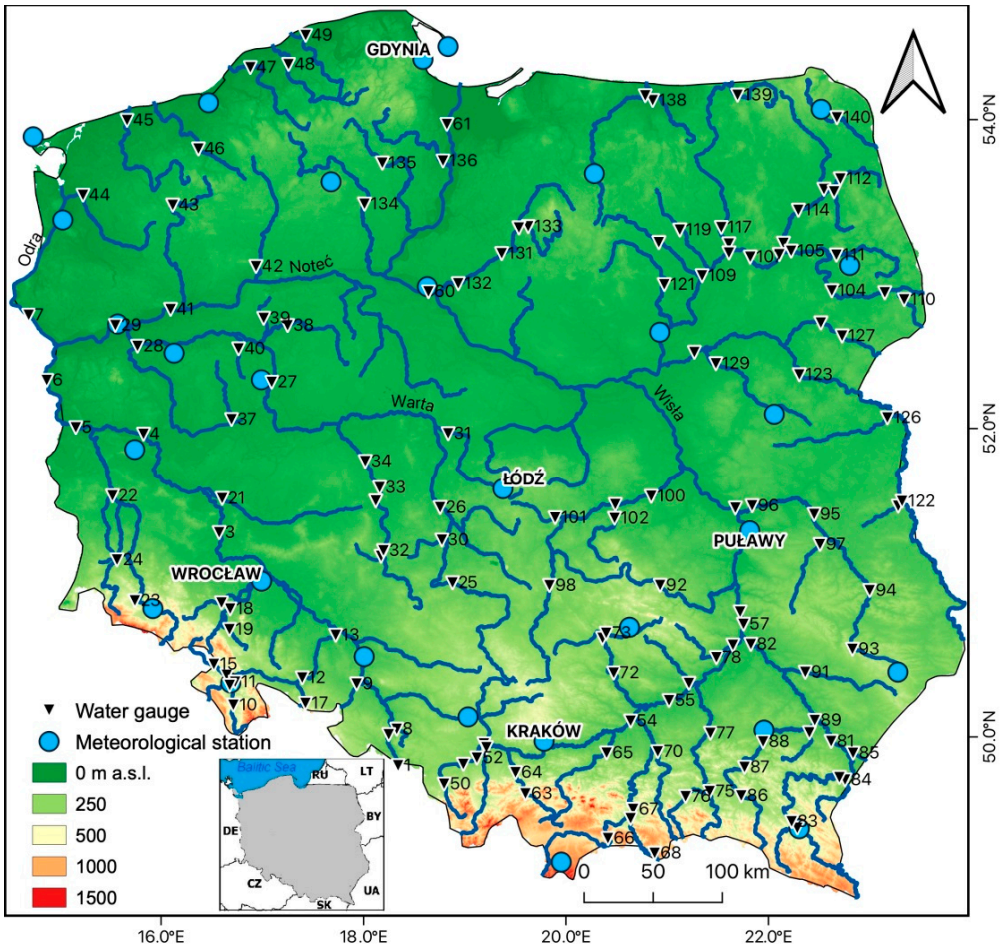

Figure 1. Position of the analyzed water gauges and meteorological stations in Poland.

The time sequences of the frequency of the macro-types of the mid-tropospheric circulation according to the Wangengejm-Girs classification, compiled by the Arctic and Antarctic Research Institute (AARI), St. Petersburg, RF, covering the period from January 1951 to March 2018 were obtained from Appendix No. 2 to the study implemented by the authors of [27]. The remaining parts of the sequences, until December 2020, were obtained directly from AARI.

Additionally, the work used the time series of the geopotential height of the isobaric surface of 500 hPa (h500) and the similar series of pressure at sea level (SLP) with a monthly resolution from selected grids. The annual values of h500 and SLP for individual grids were calculated as simple arithmetic means of monthly values in a given calendar year. Both types of data were obtained from NCEP/NCAR reanalysis [28] and were downloaded from NOAA/OAR/ESRL PSL, Boulder, Colorado, USA, from their website at https://psl.noaa.gov/data/gridded/data.ncep.reanalysis.pressure.html (accessed on 12 January 2021).

3. Methods

The values of field evaporation (Ev, mm of water column equivalent) in a given month from the area of Poland were calculated using the Ivanov formula (after [29]):

$$Ev = 0.0018 \times (25 + t)^2 \times (100 - f), \quad (1)$$

where t is the monthly average temperature (°C), f is the monthly relative humidity (%), in which arguments of function (1) are the area means of T_{PL} and f_{PL}. Annual field evaporation was calculated as the sum of monthly evaporation. The method of estimating field evaporation using the formula proposed by Ivanov is considered to give the most realistic results and performs satisfactorily in Poland (e.g., [3,30–32]). Using a series of annual Ev values, the approximate water balance in a given calendar year was estimated as the difference between annual precipitation (P_{PL}) and annual evaporation (Ev), without taking into account retention.

The threshold level method is one of the most widely used in hydrological analyses of low flows. In this method, low flow is defined as the period during which the flows are equal to or lower than the adopted threshold value [33]. However, the criteria for establishing that threshold values are not clearly defined in scientific literature, and are taken arbitrarily depend on the researcher. Among the statistical criteria, the value of the Q_p percentile with the assumed exceedance probability is determined, calculated on the basis of the sum flow curve (integral curve) plotted at the individual water gauge for the studied period. The most common *p*-values are 90 and 95 [34].

In our research, we used the 10th percentile (Q_{10}) from the sum flow curve with the lower values, which corresponds to the 90th percentile (Q_{90}) from the sum flow curve with the higher values. The low-flow periods were characterized with the use of the number of days with low flows (ND_{LF}) below a threshold value, which was adopted as the 0.1 (10%) percentile (Q_{10}) from the set of daily flows in 1951–2020. The duration of low flows was calculated for the entire multi-annual period 1951–2020 and two sub-periods: Before (1951–1988) and after climate change (1988–2020). In the next stage of the analysis, the change trends in the number of days with flows below Q_{10} detected at the respective water gauges and their statistical significances were determined. The differences in the duration of low flows below Q_{10} between the period after climate change (1988–2020) and before it (1951–1988) were also calculated.

In order to get in more detail into the structure of ND_{LF} variance and to explain the connections between ND_{LF} at individual water gauges, the set of the ND_{LF} time series was analyzed with the help of the Principal Component (PC) method. The use of the PC method is justified by the fact that the time series of the number of days with low flows at individual water gauges shows the differentiated strength of correlation, the vast majority of which are statistically significant and highly significant. Additionally, in this study, the long series of data are correlated with each other, and the PC method allows for the reduction in the number of analyzed variables, and for the detection of the variance structure and general regularities in the relationships between these variables.

The variance structure of ND_{LF} was determined based on the analysis of the eigenvector relationships between five area climatic elements (precipitation—P_{PL}, temperature—T_{PL}, relative humidity—f_{PL}, general cloudiness—N_{PL}, sunshine duration—SD_{PL}) and the annual area evaporation (Ev_{PL}) and two large-scale climate indicators, i.e., the winter (DJFM) Hurrell NAO index (PC-based) and the DG_{3L} index, informing about the intensity of thermohaline circulation in the North Atlantic.

The mathematical and statistical processing of analysis results employed the statistical procedures included in the following software: Excel (Microsoft, Redmond, WA, USA) and Statistica 13 (TIBCO Software Inc., Palo Alto, CA, USA). The implementation of the graphic form employed QGIS (3.6.2. Noosa) and Surfer 10 (Microsoft, Redmond, WA, USA) software. The kriging procedure was applied for the construction of isolinear maps.

4. Changes in Climatic Conditions in 1951–2020 and Their Scope

4.1. Changes in Macro-Circulation Conditions

The macro-circulation conditions in the Atlantic-Eurasian circulation sector are determined by the frequency of the mid-tropospheric circulation macro-types (500 hPa) W, E, and C, according to the Wangengejm-Girs classification [35,36]. The annual frequency of these macro-types for the periods of several or several dozen years maintains certain features of the stability of the proportions between them, with the dominance of a specific macro-type or the dominance of one and sub-dominance of another macro-type, creating the so-called "circulation epochs" [37].

In the 70 years of the multi-annual period 1951–2020 analyzed in this study, the macro-circulation conditions in the Atlantic-Eurasian circulation sector changed twice (Figure 2). In 1965–1966, there was a transition from the circulation epoch E + C into epoch E, and in 1989–1990, from epoch E into epoch W [38]. Similar boundaries between these circulation epochs, showing a 1–2-year shift in time in relation to the separations proposed by the authors of [38], were determined by the authors of [39,40], who used different methods of their delimitation. (The transition from one circulation epoch to the next one is not immediate and takes several (3–4) years, in which the frequency of the dominant macro-type decreases to the long-term mean values and then drops below this value, and is replaced by another macro-type, gradually increasing above its long-term average. Depending on the adopted delimitation method and the length of the analyzed datasets, researchers may obtain different moments of "transition" from one to the next epoch).

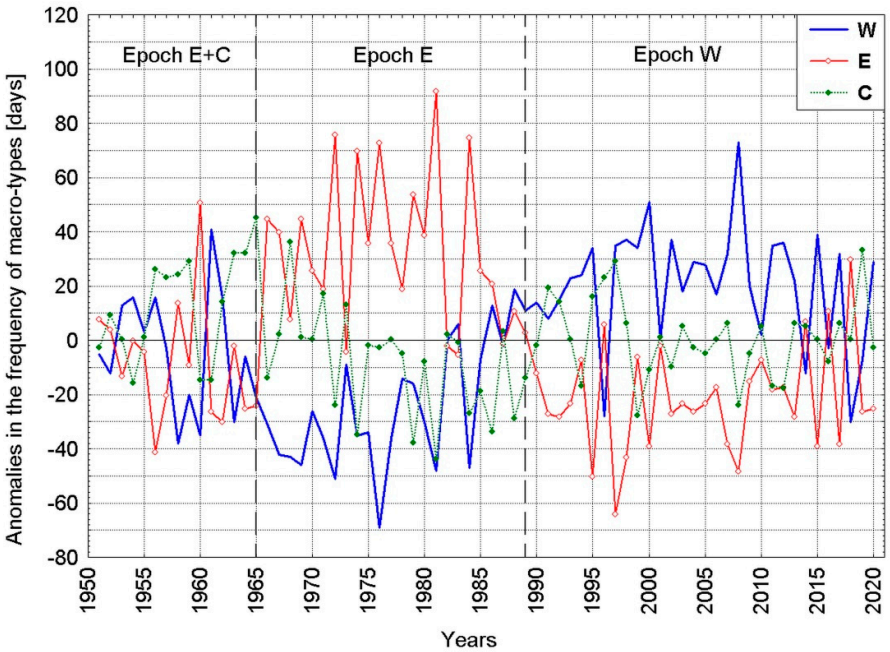

Figure 2. The course of the anomaly in the annual frequency of the mid-tropospheric circulation macro-types W, E, and C, according to the Wangengejm-Girs classification, in 1951–2020. Anomalies calculated based on averages from 1951–2000. Boundaries of the circulation epochs are marked with the vertical dashed lines.

After 1988, the frequency of the meridional macro-type E fell sharply below its long-term mean value, while the frequency of the zonal macro-type W increased noticeably, significantly exceeding the long-term mean values, and the frequency of macro-type C remained slightly below its long-term average; this state lasted until 2020 (Figure 2). The transition from the circulation epoch E into epoch W in 1987–1989 resulted in an abrupt change in the structure of the macro-types frequency.

Since the change in the structure of macro-types between individual circulation epochs was abrupt, it also forced simultaneous abrupt changes in the value of climatic elements, as the variability of the mid-tropospheric circulation controls the variability of the lower atmospheric circulation (SLP), and thus the weather structure. These changes in the mean values of climatic elements and their variability ranges, in the light of the definition of the climate by the authors of [41], can be interpreted as climate change.

4.2. Changes in the Course of Climatic Elements in Poland in 1951–2000

The analysis of annual changes in the area values of climatic elements and their distributions in respective circulation epochs shows that their changes between the circulation epoch E + C and epoch E (1965–1966), although noticeable, in most cases were not statistically significant. On the other hand, the changes of most climatic elements during the transition from the circulation epoch E into epoch W, which took place between 1987 and 1989, were highly significant. This prompts the conclusion that climate change occurred in these years.

In this paper, the characteristics of changes in the course of climatic elements will be limited to their presentation on the scale of the annual area averages and to these elements that have the strongest impact on the water balance. The value of the annual average of a given element is a synthesis of monthly and seasonal changes taking place in a given year.

Air temperature in the multi-annual period 1951–1988, despite the change in circulation epochs from E + C into E and significant inter-annual variability, did not show statistically significant long-term changes. Its trend in 1951–1988 was nearly zero (-0.0025 (± 0.0105) °C $\times$ year^{-1}, $p = 0.813$). Between 1987 and 1989, there was a "leap" in the temperature increase by slightly more than 1°, and then a positive, statistically significant trend appeared in its course (+0.0420 (± 0.0123) °C $\times$ year^{-1}, $p = 0.002$). The course of temperature noticeably changed after 1988 (see Figure 3A), which is particularly visible in the course of the lower envelope of its variability band. The annual temperature course indicates that until 1988, despite very high inter-annual variability, no increase in temperature over Poland was observed (analysis of the temperature changes in Poland covering the period 1931–2020 shows that in 1931–1988 (58 years), despite very high inter-annual variability, the trend was zero), and a warming exceeding 2° by 2020, did not begin until after 1988.

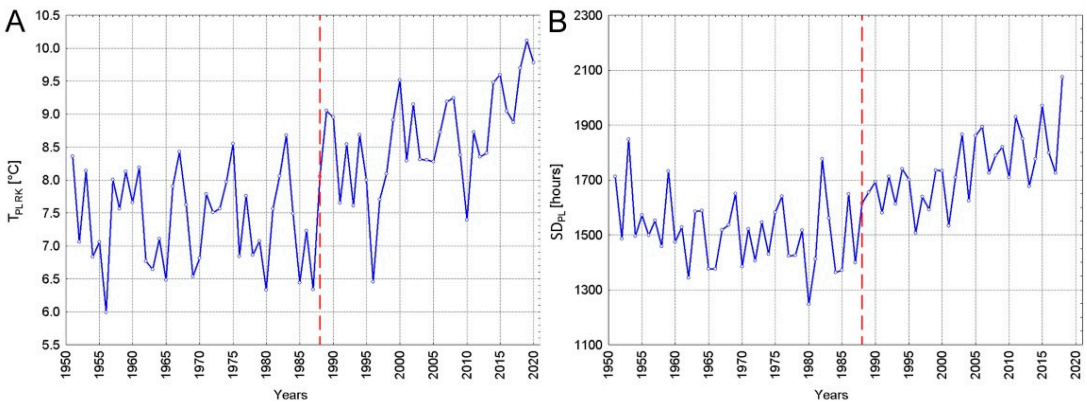

Figure 3. Courses of the annual area air temperature (T_{PL}) (**A**) and sunshine duration (SD_{PL}) (**B**) in Poland in 1951–2020. The year 1988, when the courses changed and a positive trend appeared, is marked with the vertical dashed line.

Changes in sunshine duration were similar to the temperature changes. The time series is also non-stationary, and the period of its discontinuity can be found between 1987 and 1989 (Figure 3B), when there was a clear "leap" in the course of sunshine duration and then a positive trend appeared. It occurred along with the transition from the circulation epoch E into epoch W, while the transition from the circulation epoch E + C into epoch E

did not cause statistically significant changes in the annual sunshine duration. In 1951–1988, the annual sunshine duration trend was negative (−2.76 (±1.88) hours × year^{-1}) and statistically insignificant (p = 0.150), while in 1988–2018, the trend became positive (+9.11 (±2.02) hours × year^{-1}) and highly significant (p << 0.001). Even a stronger relative increase in sunshine duration in 1987–1989 can be concluded when considering the changes in sunshine duration in the warm half-year (April–September), i.e., during the "long-day months". In the course of the warm half-year sunshine duration, both the value of the "leap" and the positive trend after 1988 are stronger than the course of annual values. This indicates that the fundamental changes in sunshine duration between the two sub-periods took place in the warm half-year [42].

The changes in the range of variability in temperature and sunshine duration between the two sub-periods are significantly strong, in which the values of these two climatic elements in each analyzed sub-period resulted in statistically separate populations (Figure 4).

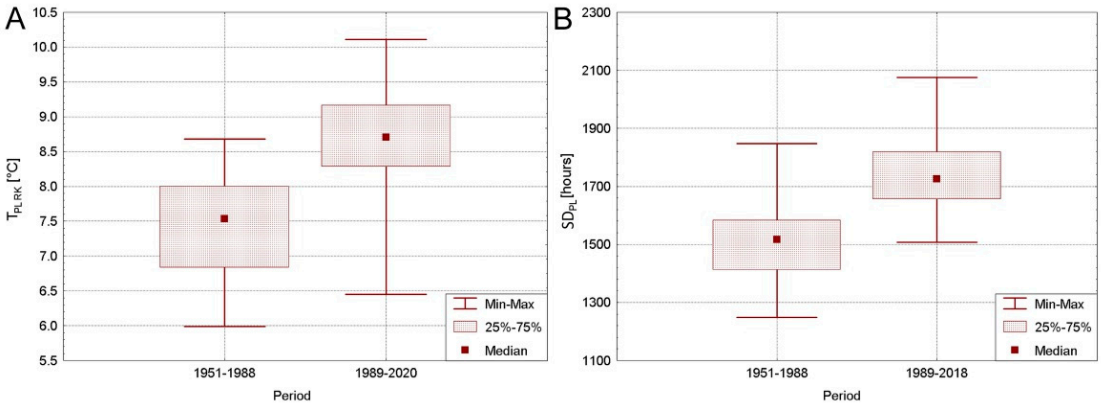

Figure 4. Ranges of variability of the annual area air temperature (T_{PL}) (**A**) and sunshine duration (SD_{PL}) (**B**) in Poland in sub-periods 1951–1988 and 1989–2020.

Moreover, the annual area relative humidity in Poland, that very strongly correlated with T_{PL} and SD_{PL}, shows clear differentiation in the analyzed two sub-periods. While the mean values of f_{PL} in these sub-periods differ slightly (80.85 and 79.37%), the distributions of the f_{PL} values are clearly different. The analysis of differences between the means of the sub-periods 1951–1988 and 1989–2020 shows that the differences between these means are highly significant (p = 0.0001 in the one-tailed test and 0.0003 in the two-tailed test).

The course of the annual area precipitation totals in the whole analyzed period shows a weak and statistically insignificant positive trend (+0.63 (±0.48) mm × year^{-1}, p = 0.191; Figure 5), and does not show discontinuities in 1987–1989, despite a temporary decrease in the annual precipitation totals in 1986–1993. The calculated differences between the mean annual precipitation in the two sub-periods (617.0 and 632.2 mm, respectively) are insignificant. On the other hand, the distribution of the annual precipitation totals changed in the second sub-period compared to the first sub-period: The annual precipitation maxima increased to 843 mm in 1989–2020 compared to 780.3 mm in 1951–1988, and the annual minima to 506.8 mm compared to 446.1 mm, respectively. This change in the range of variability of the maxima can be explained by the increased frequency of convective precipitation in the sub-period 1989–2020, with significant sums of precipitation recorded during individual rainfall episodes.

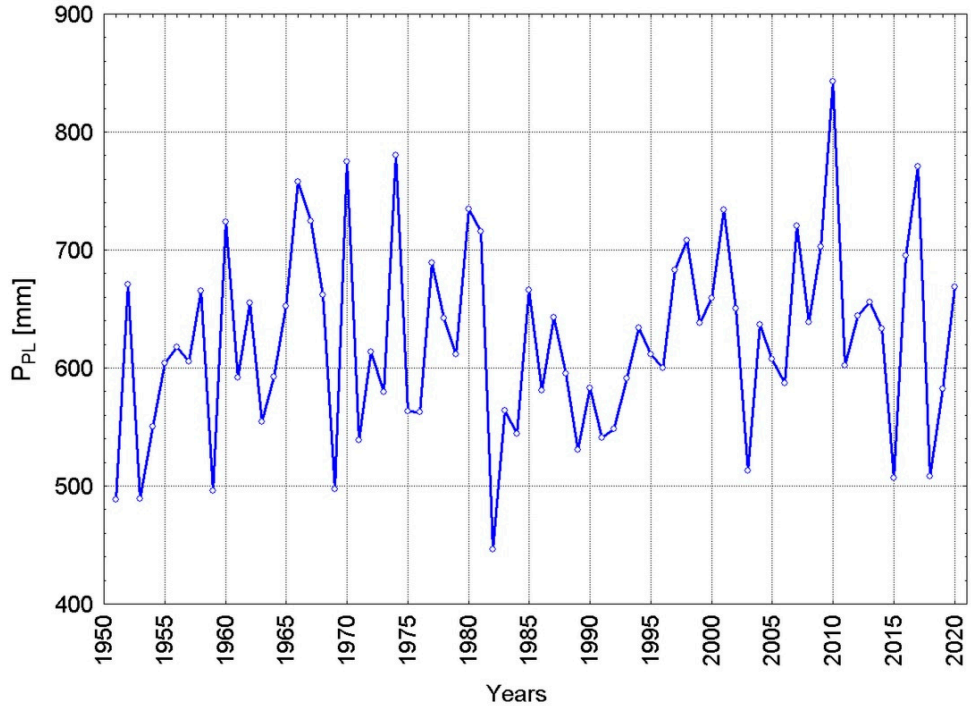

Figure 5. Course of the annual area precipitation (P_{PL}) in Poland in 1951–2020.

4.3. Changes in the Water Balance

The annual area evaporation (Ev_{PL}) calculated with the use of method proposed by Ivanov in the two sub-periods show significant differences: In 1951–1988, it was an average of 493.4 mm, while in 1989–2020, this value increased to 579.1 mm. The variability ranges of the inter-annual evaporation also changed. In 1951–1988, the minimum Ev_{PL} reached 401.8, and the maximum 602.8 mm, while in 1989–2020, both extreme values increased: The minimum Ev_{PL} was 451.1 mm, and the maximum 728.0 mm. Therefore, in 1989–2020, the amount of water losses on evaporation increased very strongly in Poland compared to 1951–1988, and the variability of the evaporation values calculated for each of these sub-periods also created two separate populations (Figure 6A).

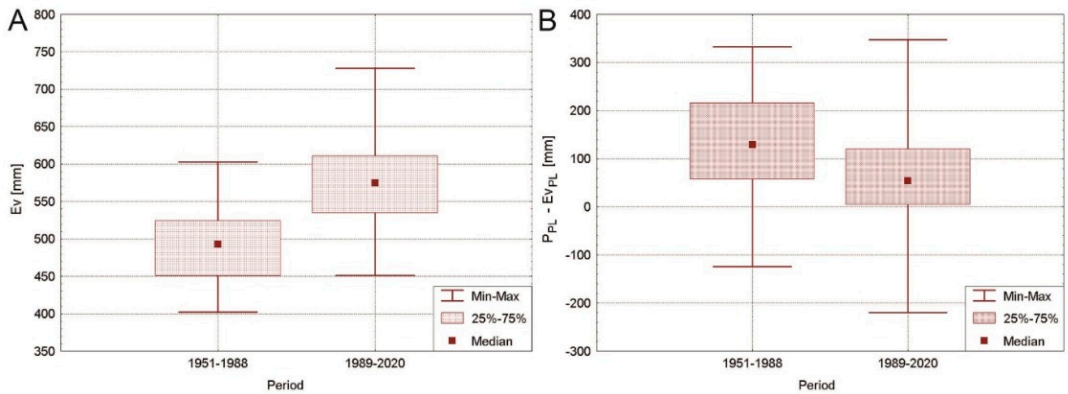

Figure 6. Ranges of variability of the annual area field evaporation (Ev) (**A**) and simplified water balance (**B**) in Poland in sub-periods 1951–1988 and 1989–2020.

The strong and highly significant increase in field evaporation (Ev_{PL}) in 1989–2020, in the face of significant, but practically non-directional changes in annual precipitation totals in the same period, raises the question about the value of the simplified annual water balance (the simplified water balance is considered as the difference between the annual precipitation and the annual evaporation (P_{PL}–Ev_{PL}). It is "simplified" in the sense that the non-quantifiable

retention is not included) in Poland. The calculated difference between the annual area precipitation totals and the annual area evaporation (P_{PL}–Ev_{PL}) shows that in years with a reduced precipitation this balance reached slightly positive values (<100 mm), while in some other years even negative values (Figure 7). While the difference in the number of years with the negative water balance in both sub-periods is not significant (6 and 8 years, respectively), the fundamental change occurs in the distribution of the number of years with specific ranges of the water balance. In the first sub-period (1951–1988) there were 12 years, in which the excess of precipitation over the evaporation per year exceeded 200 mm, while in the second sub-period (1989–2020) there were only 2 years (Figure 5). Moreover, there are clear differences between these sub-periods in terms of the number of years, in which the simplified positive water balance was between 0 and 100 m (11 and 15 years, respectively).

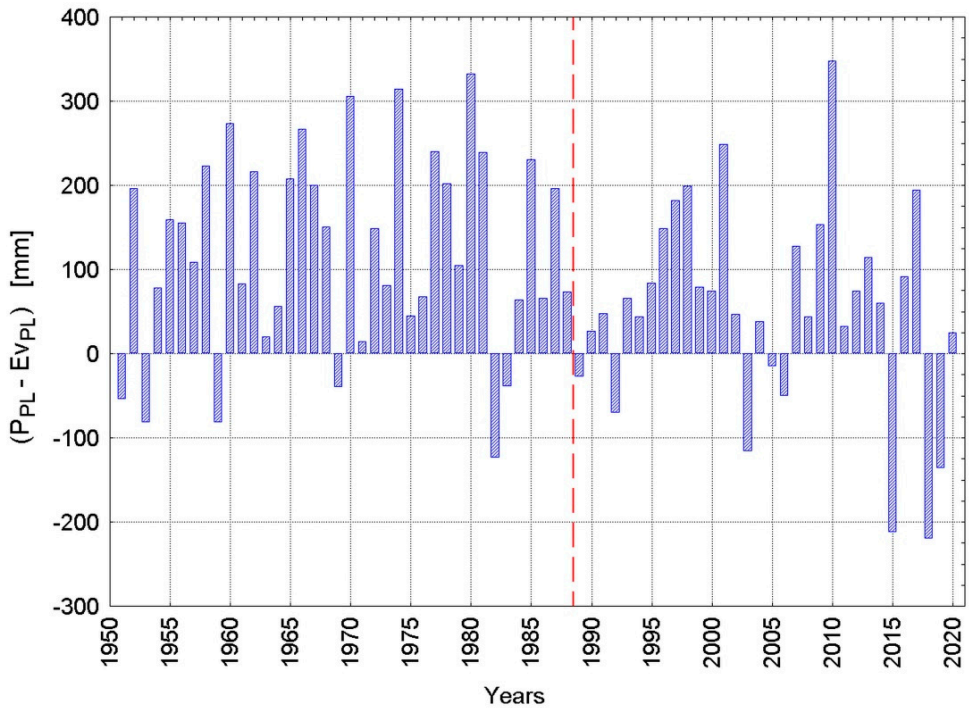

Figure 7. Values of the simplified annual area water balance (mm) in 1951–2020. The sub-periods 1951–1988 and 1989–2020 are separated with the vertical dashed line.

These and other, not discussed here, differences in the distribution of difference between the annual area precipitation and the annual area evaporation (Figure 6A) result in statistically significant differences between the water balance in the two sub-periods (Figure 6B). The balance changed toward a decrease in its positive values in the sub-period following the climate change (in 1951–1988: Lower quartile 56.6 mm, upper quartile 215.8 mm, in 1989–2020: Lower quartile 24.5 mm, upper quartile 114.6 mm), and a strong increase in its amplitude, mainly due to the deepening of the minimum.

This allows us to conclude that along with the climate change that occurred in 1987–1989, despite the lack of statistically significant changes in the course of annual precipitation totals, a statistically significant change in the simplified water balance also took place. The reason for these changes is the strong increase in 1988 in evaporation losses.

5. Number of Days with Low Flows (ND_{LF}) on Polish Rivers

The variability of the annual mean area number of days with low flows in Poland (ND_{LF}) in the multi-annual period 1951–2020 is significant and ranges from one (minimum) to 112 days (maximum), with an average of 35.8 days (standard deviation: $\sigma = 28.5$) and a median of 25.3 days. The distribution of ND_{LF} is different from normal, the time series is dominated by years, in which ND_{LF} is within the range of 1–20 days (24 cases) and

21–40 days (22 cases), which in total accounts for ~65.7% of the analyzed 70 years. Only three cases (~4.3%) are in the highest range of distribution (>100 days). The course of area number of days with low flows in the multi-annual period 1951–2020 is shown in Figure 8.

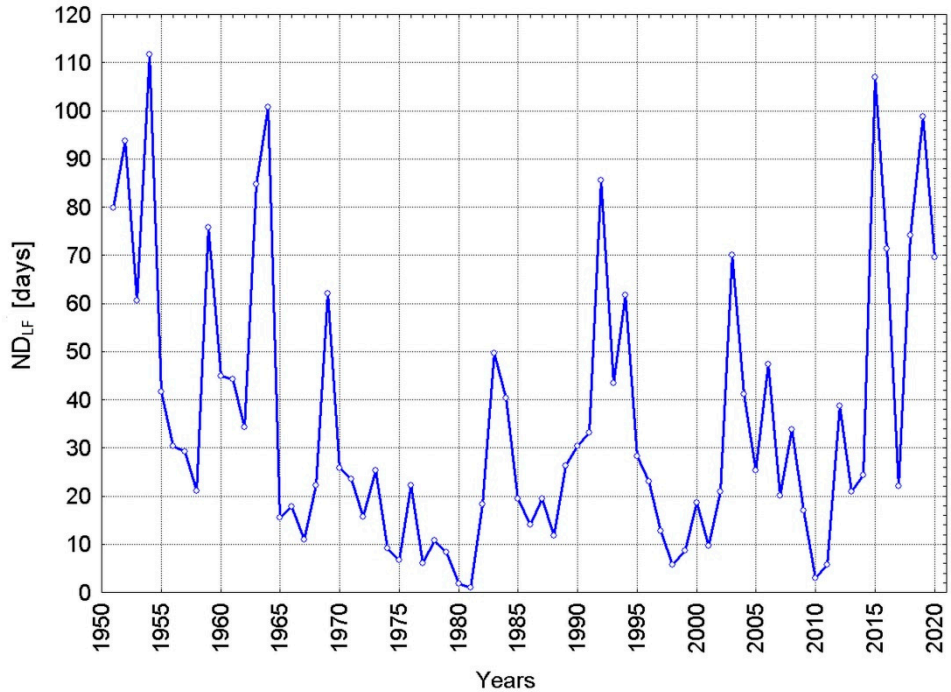

Figure 8. Course of the average number of days with low flows (ND_{LF}) in Poland in 1951–2020.

In the course of ND_{LF}, there are usually short periods (from one to several years) in which the number of days with low flows are greater than the average, separated by periods of various lengths, in which the ND_{LF} per year is lower than the average. There was an increased frequency of higher ND_{LF} values at the beginning and end of the analyzed data series. There is a weak (−0.11 (±0.17) and insignificant (p = 0.501) negative trend in the ND_{LF} series.

However, the separation of the ND_{LF} series into two parts, corresponding to the sub-period before climate change and the increased water balance (1951–1988) and the sub-period after climate change and the reduced water balance (Figure 9A), reveals some differences in the distribution of the ND_{LF} values in these sub-periods, and also a slight increase in the ND_{LF} range between the lower and upper quartiles; however, these differences are negligible. Testing of differences between the mean ND_{LF} in both sub-periods indicate that these differences are statistically insignificant. This is surprising, since if the ND_{LF} series is divided in accordance with the time intervals between the circulation epochs (Figure 9B), then both the differences in the distributions and the tests of differences between the mean ND_{LF} prove that there is a statistically significant differentiation in the respective circulation epochs.

Therefore, the result of this part of the analysis is at least ambiguous. On the one hand, it shows that the number of days with low flows clearly differs from the change in the circulation epoch E + C into epoch E, in which the differences between the climatic elements influencing the water balance between these epochs are mostly insignificant. On the other hand, it proves that the strong climate change, leading to a clear change in the water balance, is not significantly reflected in the changes in the average area of the number of days with low flows.

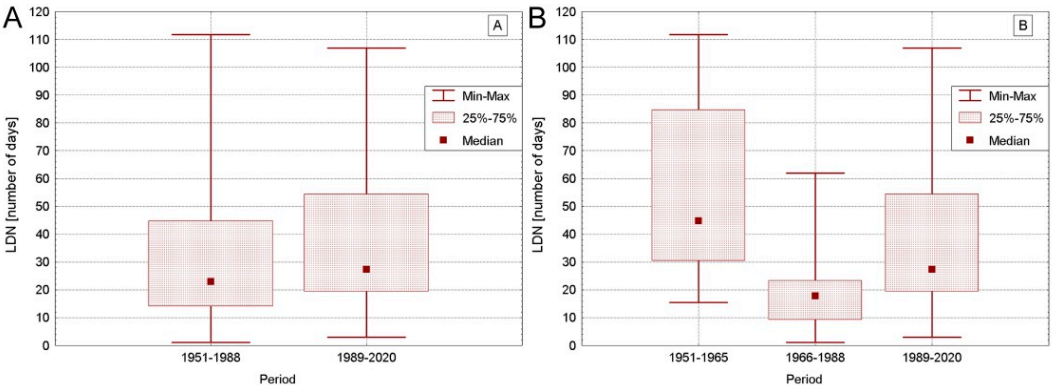

Figure 9. Ranges of variability of the average number of days with low flows (ND_{LF}) in sub-periods before (1951–1988) and after climate change (1989–2020) (**A**) and in three sub-periods corresponding to different macro-circulation epochs (**B**).

The results obtained require further clarification. In order to get in more detail into the structure of ND_{LF} variance and to explain the connections between ND_{LF} at individual water gauges, the set of the ND_{LF} time series was analyzed with the help of the principal component analysis.

5.1. Results of the Principal Component Analysis

The conducted analysis allowed for the detection of 20 principal components with factor values greater than 1.0, i.e., statistically significant, according to the Kaiser criterion. The scree test indicated that the first four main components [43] were relevant for the analysis, explaining 62.79% of the total variance of the set of analyzed variables (Table 1).

Table 1. Results of the principal component analysis of the set of ND_{LF} recorded at 140 water gauges on 83 rivers in Poland in 1951–2020.

Principal Component Number	Eigenvalue	% of Explained Variance	Cumulative Eigenvalue	Cumulative Explanation of Variance (%)
1	58.019	41.442	58.019	41.442
2	14.277	10.198	72.296	51.640
3	10.182	7.273	82.478	58.913
4	5.428	3.877	87.907	62.790

The time series of the factor values of each principal component created eigenvectors, which were then analyzed in terms of their physical meaning. The analysis shows that the first eigenvector (1 EV) is a series of standardized anomalies (deviations from the average of 140 water gauges) in ND_{LF} per year. It explains less than half of the total variance of the set, i.e., 41.4% of the total variance included in the time series of ND_{LF} recorded at 140 water gauges. The physical sense of the second eigenvector (2 EV) is the difference in the response of a certain part of the catchment to changes in water feeding in relation to 1 EV. As it can be concluded from the analysis of the distribution of points on the common areas of individual factor loads, the third and fourth eigenvectors (and the remaining ones, up to 10, not discussed in this paper) present the characteristics of regional differentiation of individual catchment groups, which are the cause of more or less distinct differences in relation to the area average.

The analysis of the eigenvector relationships between five area climatic elements (precipitation—P_{PL}, temperature—T_{PL}, relative humidity—f_{PL}, general cloudiness—N_{PL}, sunshine duration—SD_{PL}) and the annual area evaporation (Ev_{PL}) and two large-scale climate indicators, i.e., the winter (DJFM) Hurrell NAO index (PC-based) and the DG_{3L} index, that inform about the intensity of thermohaline circulation in the North Atlantic,

allowed for the clarification of a number of issues related to the shaping of the variance structure of ND_{LF}. The results of this analysis are presented in Table 2.

Table 2. Correlation coefficients between eigenvectors (EV) of ND_{LF} and the area climatic elements (P_{PL}, T_{PL}, f_{PL}, N_{PL}, SD_{PL}, Ev_{PL}), the winter NAO index (NAO_w, PC-based) and the DG_{3L} index characterizing the heat transport intensity to the north through the thermohaline circulation in the North Atlantic (1951–2020).

Eigenvector	% of Explained Variance	P_{PL}	T_{PL}	f_{PL}	N_{PL}	SD_{PL} *	Ev_{PL}	NAO_W	DG_{3L}
1 EV	41.442	**−0.48** 0.000	0.21 0.084	**−0.57** 0.000	**−0.39** 0.001	**0.35** 0.004	**0.51** 0.000	0.16 0.191	**0.45** 0.000
2 EV	10.198	−0.02 0.852	**0.56** 0.000	**−0.46** 0.000	0.01 0.971	**0.45** 0.000	**0.51** 0.000	**0.40** 0.001	**0.40** 0.001
3 EV	7.273	0.05 0.664	0.15 0.212	−0.09 0.439	0.13 0.274	0.06 0.641	0.11 0.362	**0.34** 0.004	0.21 0.084
4 EV	3.877	0.05 0.657	0.16 0.197	**0.24** 0.047	0.03 0.808	−0.17 0.162	**−0.26** 0.030	−0.15 0.205	−0.03 0.823

Note: The r value is shown in the upper row of the cell, the *p*-value (statistical significance r) is shown in the lower row; *p*-values marked with 0.000 indicate $p << 0.001$; *—the correlation coefficients calculated from the series of only 68 pairs of values (1951–2018). Significant ($p < 0.05$) correlation coefficients are marked in bold.

Both the first and second eigenvector with the same strength are positively related to the annual evaporation. The greater it is, the greater the likelihood of low flow. The first eigenvector (1 EV) is negatively related to the annual precipitation totals, general cloudiness, and relative humidity, while positively to sunshine duration. The greater the values of precipitation, cloudiness, and relative humidity, the lower the likelihood of low flows, the greater the sunshine duration, the greater the losses on evaporation, and the greater the likelihood of low flow. It should be noted that 1 EV is not significantly related to temperature. Among the large-scale climate indicators, 1 EV is significantly related only to the DG_{3L} index, which reflects the impact of changes in the thermal state of the North Atlantic on the climate of Poland, but it is not significantly related to the winter NAO index.

The second eigenvector (2 EV) shows almost no relationship with the annual precipitation and general cloudiness. It is strongly and positively related to air temperature and, stronger than 1 EV, to sunshine duration, while weaker to relative humidity. It is highly significantly related to the winter NAO index, which by regulating the duration of snow cover [44–46], with a negative sign, has a strong impact on river flows in some parts of Poland [47–52], and with a positive sign on the size of winter field evaporation [42,53]. The 2 EV is slightly less than 1 EV related to the DG_{3L} index, which in Poland regulates, among others, the frequency of droughts and, to a lesser extent, the long-term variability of annual river flows [54,55]. Therefore, the variability of 2 EV does not involve the main factor on the "revenue" side of the water balance, i.e., precipitation, but only the factors determining the size of the balance losses.

This allows us to conclude that the variability of 1 and 2 EV is strongly, albeit in different ways, related to the variability of climatic conditions, including variability of the large-scale circulation conditions, and these factors jointly control their variability.

The last eigenvector showing the influence of large-scale circulation indices is 3 EV, which shows the relationship with NAO. In the case of subsequent eigenvectors—4 EV and following—the large-scale influences become negligible, and the relationships with the elements of area climate usually lose their significance, as well.

While the first eigenvector is positively correlated with all 140 series of ND_{LF} recorded at individual water gauges (although not significantly in every case), the second and subsequent eigenvectors change their signs in correlation with the individual series of specific groups of water gauges and/or individual water gauges. As the sequence number of the eigenvector increases, the degree of fragmentation of the plot increases, dividing it into sections with positive and negative values of the correlation coefficient (Figure 10). As

the water gauges identifiers (ordinal numbers) are arranged geographically according to the location of the catchment area, it clearly indicates the increasing regional and local factors in shaping the diversity of the whole set in relation to the mean, along with the increase in the eigenvector sequence number and its decrease in its importance in explaining the total variance of the set.

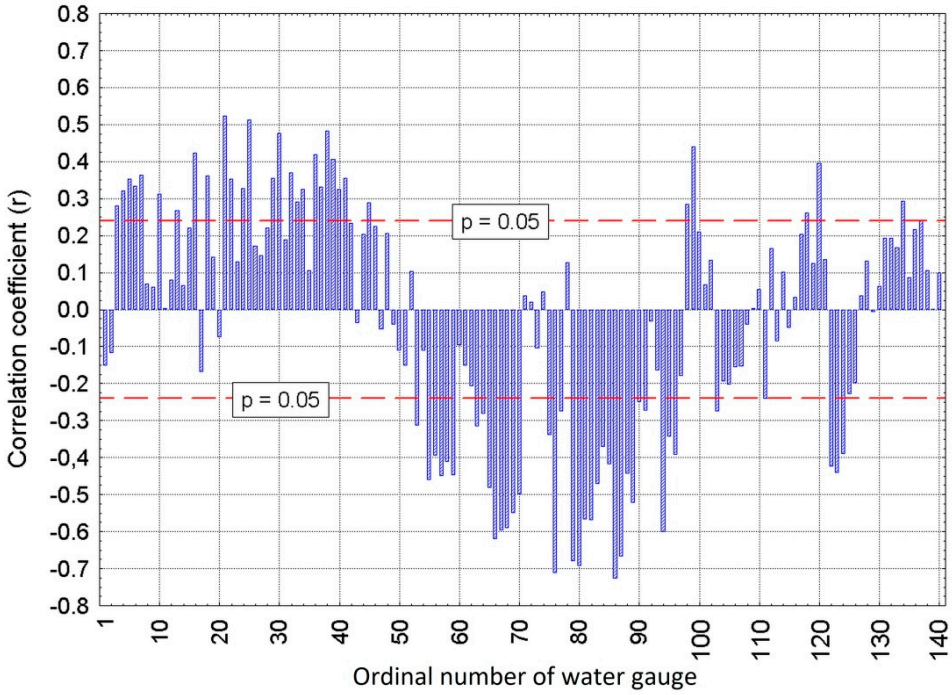

Figure 10. Correlation coefficients (r) between 2 EV of the set of ND_{LF} and ND_{LF} per year at individual water gauges in Poland in 1951–2020. The lower boundary of statistical significance (p = 0.05) is marked with the dashed line.

To date, it can be assumed that the effect of the not considered factor of the regional differentiation, proves that the statistical analysis of the ND_{LF} relationship with climatic elements, treated as uniform on the country (Poland) scale, does not detect statistically significant changes in ND_{LF} that occur along with the change in climatic conditions (see Figure 9A,B). This requires further analysis of the spatial distribution of changes in ND_{LF} at individual water gauges, considered in a function of time.

5.2. Spatial Analysis of the Relationship between the Number of Days with Low Flows (ND_{LF}) and Changes in Climatic Conditions

The spatial analysis of the relationship was carried out with the help of the cartographic method. For this purpose, the time series of ND_{LF} from all 140 water gauges with their strictly defined geographical location was investigated. The spatial distribution of the areas through which the flowing rivers have a certain average ND_{LF} per year in Poland in the multi-annual period 1951–2020 is presented in Figure 11.

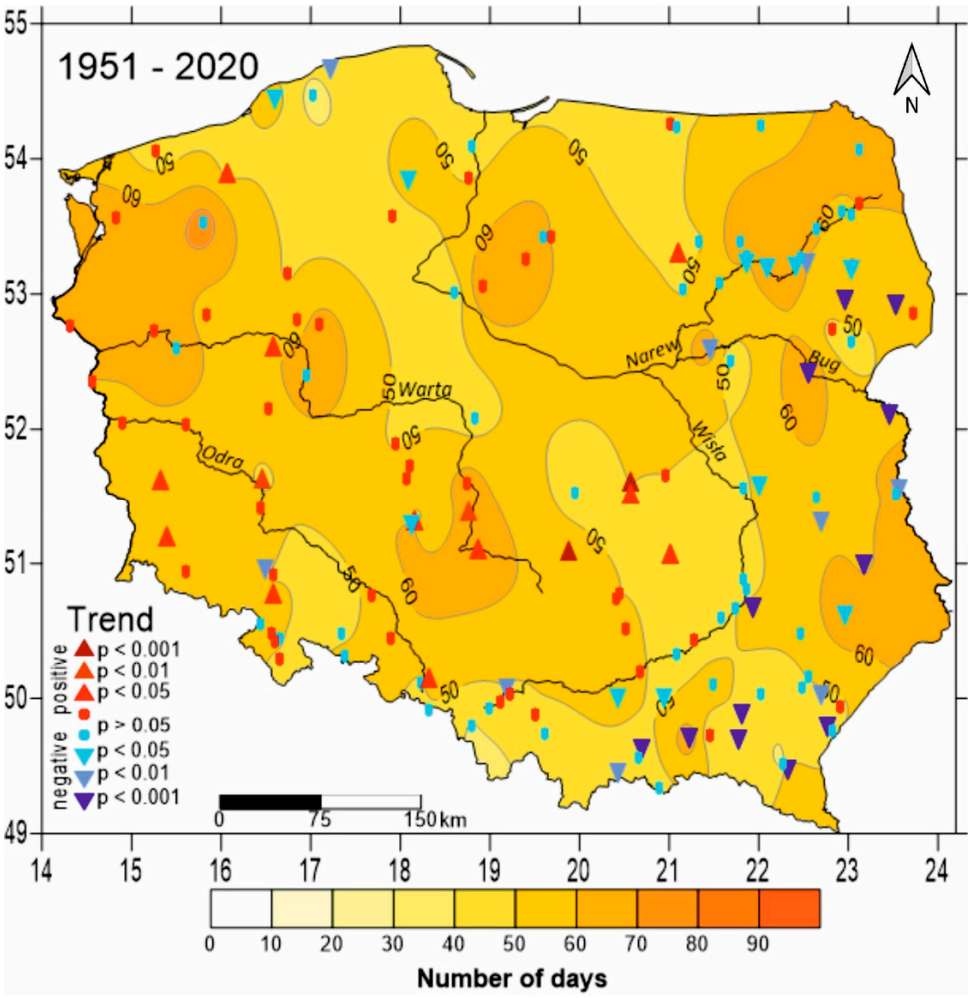

Figure 11. Spatial distribution of ND_{LF} and the trends of changes in 1951–2020 with their statistical significance (*p*).

The spatial distribution of ND_{LF} shows quite significant differentiation, creating bands of increasing and decreasing values with the NW–SE course. The increasing number of ND_{LF} is reflected in a kind of "centers" (>60 days a year) marking the axes of these bands. The first band extends from the area of Western Pomerania, through Greater Poland, the Kraków-Częstochowa Upland, to the upper reaches of the Vistula River. The second one stretches from the southern end of the Kashubian Lake District (Kociewie), through the Chełmno and Dobrzyń Land to the eastern part of the Lublin Upland. The third band can be distinguished in the eastern part of the Masurian Lake District and the Suwałki Lake District, and is most likely a part of a longer zone, the continuation of which is located beyond the country borders. The studied trends of changes in ND_{LF} in 1951–2020 (Figure 11) show, despite their mosaic distribution, mostly downward tendencies in the north-eastern and eastern part of Poland, and mostly upward tendencies in its western and south-western parts. The spatial distribution of ND_{LF} obtained for the respective sub-periods—before the climate change (1951–1988) and after it (1988–2020)—proves that in the whole analyzed multi-annual period 1951–2020 they form two different patterns (Figure 12). There was a clear change in the spatial distribution of the areas of increased frequency of ND_{LF} between these sub-periods.

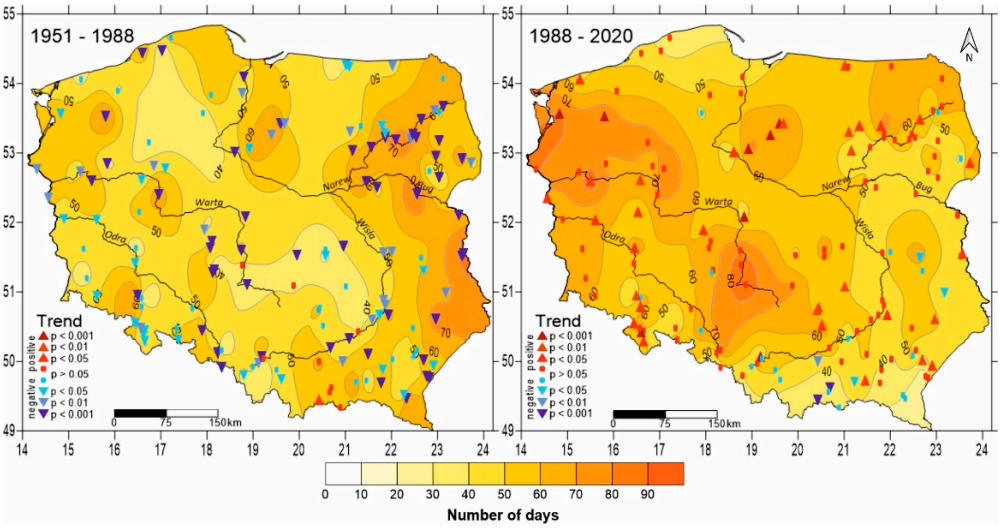

Figure 12. Spatial distribution of ND_{LF} and the trends of changes in 1951–1988 and 1988–2020. Explanations as in Figure 11.

In 1951–1988, the areas with the highest ND_{LF} included rivers located in the eastern part of Poland: From the eastern part of the Masurian Lake District to the southern edge of the Lublin region. In that area, the average ND_{LF} per year exceeded 50 days, and in its relatively large parts, it exceeded 70 days. At the same time, in the western and south-western parts of Poland, there were only single rivers, on which ND_{LF} exceeded 50 days per year, with the maximum >60 days on the Drawa River and the middle Warta River. In the rest of the country, the average ND_{LF} was within the range of 40–50 days per year, while in quite large areas (e.g., central Pomerania, the zone from the upper Warta to the Vistula in the Nida-Połaniec estuary) it was less than 40 days. In this period, negative trends in Poland dominated, most of which were statistically highly significant.

Along with the climate change an abrupt change in the spatial distribution of days with low flows in Poland can be concluded. In 1988–2020, areas with the maximum ND_{LF} were located in western and south-western Poland (Figure 11); in the lower reaches of the Odra River and in the upper reaches of the Warta River, the average ND_{LF} exceeded 80 days per year. On almost all rivers of Central and Eastern Poland, ND_{LF} was greater than 50 days per year. In that period, positive trends in ND_{LF} prevailed, with positive trends of the highest significance ($p < 0.001$) on rivers located in Western Pomerania, in the upper reaches of the Warta River and on the Drwęca River in the Vistula River basin. Negative trends in ND_{LF} in more continuous areas were detected only on the Carpathian tributaries of the upper Vistula River basin and on the middle and lower Wieprz River in the Lublin region.

The calculated difference between the average ND_{LF} per year between the sub-period after climate change (1988–2020) and the sub-period before it (1951–1988) (Figure 13) showed that ND_{LF} increased in approximately 2/3 of the area of Poland. The strongest increase took place on the upper Noteć and Warta rivers, where the average ND_{LF} increased by over 30 days.

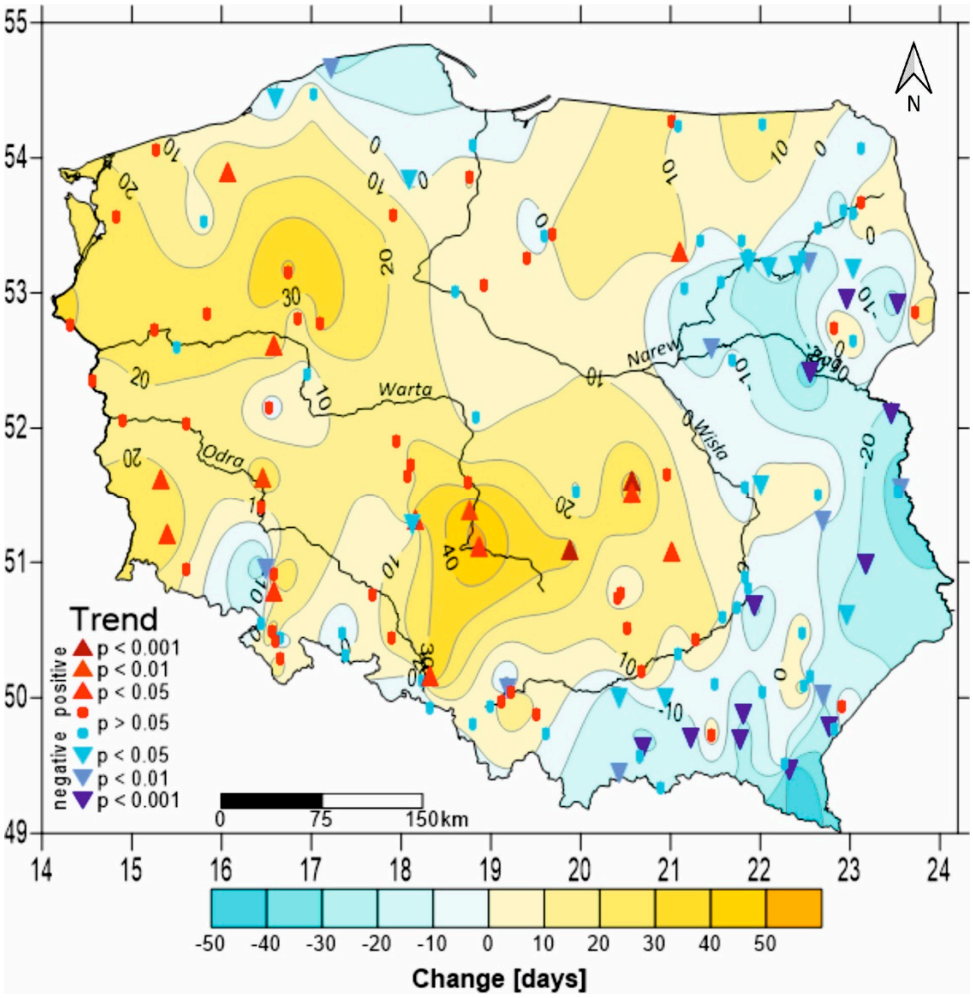

Figure 13. Spatial distribution of changes in ND_{LF} between 1988–2020 (after climate change) and 1951–1988 (before climate change in 1987–1989) and trends of changes in 1951–2020 with their statistical significance (*p*).

Continuous areas, in which ND_{LF} decreased, include rivers located in the eastern part of the Vistula River basin, from the Narew River in the northeast to the Raba River, which is a Carpathian tributary of the upper Vistula.

Generally, the analysis of the spatial distribution of ND_{LF} clearly shows that along with the climate change and the change in the water balance in Poland, abrupt changes occurred both in the number of days with low flows and in the spatial distribution of their occurrence (Figures 12 and 13).

6. Discussion

Comparing the results of the cartographic and statistical analyses allows for explaining the reasons why the statistical analysis did not detect statistically significant changes in ND_{LF} in Poland. This analysis was based on a series of averaged values of ND_{LF} for all 140 water gauges. In a situation where during the period of increasing evaporation and decreasing water balance (1988–2020), the changes were multi-directional—in a part of the analyzed area ND_{LF} was increasing and in another part decreasing. With area averaging, opposing trends were mutually compensated and the obtained value of the area average could not properly characterize the spatially diversified course of the studied process.

The main results of the conducted analyses indicate that the observed climate change consisted of a sudden increase in sunshine duration and air temperature, a decrease in relative humidity, leading to an equally strong increase in field evaporation (Figure 7A). In

the conditions of significant variability of the annual precipitation totals, this resulted in negative changes in the water balance (Figures 6 and 7B). This, in turn, caused a change in the structure of river flow in Poland (Figures 12 and 13). Along with the decrease in the water balance, ND_{LF} (below Q_{10}) increased in most areas of Poland. Determining the significance level of this increase requires more detailed research, and for this purpose a comparison of differences between the means seems to be more appropriate than the analysis of linear trends.

The greatest increase in ND_{LF} in 1988–2020 was concluded on rivers in western and south-western Poland, while in the same sub-period the number of these days in eastern Poland decreased compared to the preceding sub-period (1951–1988).

The reason for the change in the values of climatic elements that led to climate change was the change in macro-circulation conditions—the transition from the circulation epoch E + C into epoch E, and then from the circulation epoch E into epoch W. Along with the transition from the circulation epoch E into epoch W, not only the values of climatic elements changed, but also the weather structure over Poland was modified. The structure of weather over a given area is determined by the frequency of occurrence of upper ridges and upper troughs (500 hPa) above it [56,57]. To the east of the axis of the upper ridge in the lower troposphere (850–1000 hPa) low-mobility anti-cyclones are formed, and on the border of the eastern part of the upper trough and the western part of the upper ridge cyclones are formed, which then travel toward the top of the wave and then, entering the cool air of the upper trough, they fill up. The anti-cyclonal weather is associated with the occurrence of anti-cyclones over a given area. This is the intra-mass weather characterized by increased sunshine duration and air temperature, reduced cloudiness, and decreased precipitation. The occurrence of the cyclonic system (low) is related to the occurrence of a group of cyclonic weather over a given area. In addition to the intra-mass weather is the frontal weather, characterized by high cloudiness, long-term precipitation, high humidity, very limited sunshine duration, and lower air temperature in the warm half-year.

The Wangengejm-Girs macro-types are nothing but long waves in the mid-troposphere. The macro-type W is characterized by a long wavelength (wavenumber 4), with the upper ridge "stretched" from the eastern North Atlantic to Central Europe, the axis of which is most often located over Western Europe (~5° W–5° E). The macro-type E represents a large-amplitude wave with an upper trough over the eastern North Atlantic and Western Europe and an upper ridge, the axis of which is located over the central part of European Russia (~35°–45° E). When this macro-type occurs, the border between the upper trough and the upper ridge is most often situated between 10° and 20° E [27,37], i.e., above Poland. This factor explains the changes in the spatial distribution of ND_{LF} observed at the same time over Poland (Figures 12 and 13). In 1951–1988, due to the stronger or weaker dominance of the frequency of macro-type E, the eastern part of Poland was more often under the influence of the western edge of the anti-cyclones (highs) from Russia than its western part. Therefore, the frequency of occurrence of water shortages, and thus the occurrence of low flows, was greater over eastern than western Poland, which was located in the zone of an increased frequency of cyclonic weather.

With the transition into the circulation epoch W, there was a significant increase in the frequency of occurrence of the upper ridge axis over Western Europe (~5° W–5° E). Therefore, Poland was more frequently situated on the eastern extremities of the anti-cyclones located above western Europe or the eastern periphery of the vast ridge of the Azores High. The increase in the frequency of the anti-cyclonal weather in this situation was significantly more pronounced over the western than eastern Poland, becoming the cause of a significant increase in the part of "losses" of the water balance and the frequency of low flows in the western part of Poland.

Herein, the expressed assessments of the role of the macro-type W in shaping ND_{LF}—and more generally—the relationship between the reduced runoff of Polish rivers and the increase in the frequency of macro-type W, is contradictory to the opinion expressed by [58], who based on the data from 1901–1965, found that the flows of Polish rivers increased with the increase

in the frequency of macro-type W according to the Wangengejm-Girs classification, and the change in the frequency of the macro-type was conditioned by changes in the solar cycles (the Wolf numbers). Studies on the frequency of macro-types of the mid-tropospheric circulation did not confirm (e.g., [27]) the relationship between changes in the frequency of macro-types and changes in the number of sunspots, or more generally—the relationship between changes in the circulation epochs and the 11–13-year cycle of the solar changes. The quality of the initial data (on the frequency of macro-types) and the method of their integration carried out by [58], which were the means calculated for each of the solar cycles, is questionable. Recent studies (e.g., [54,55] as well as this research) have proved that with the increase in the frequency of macro-type W, the flows of Polish rivers do not increase, but decrease.

7. Conclusions

In this study, the daily discharges observed at 140 river gauges on 83 rivers and the series of annual air temperature (T), annual precipitation totals (P), annual values of general cloudiness (N, 1/8), and annual values of relative humidity (f, %) were analyzed. The values of the above-mentioned climatic elements constituted the area averages of 28 stations relatively evenly distributed in Poland. The datasets were used to determine the change in climatic conditions and the duration and trend of changes in the number of days with low flows in the multi-annual period 1951–2020 and in two sub-periods: Before climate change (1951–1988) and after it (1988–2020).

The following conclusions can be drawn based on the results obtained:

(1) In 1987–1989, there was an abrupt change in climatic conditions in Poland.
(2) Climate change in Poland was caused by macro-circulation conditions, controlled by changes in the intensity of thermohaline circulation in the North Atlantic (NA THC).
(3) Climate change consisted of an abrupt increase in sunshine duration and air temperature, and a decrease in relative humidity after 1988. Along with the lack of changes in precipitation totals, characterized by a strong yearly variability, and an increase in field evaporation, it led to noticeable changes in the water balance.
(4) In 1951–2020, the average number of ND_{FL} days was from 30 to 70, with the dominance of upward trends on rivers in central and western Poland and negative trends on the southern and eastern tributaries of the Vistula River.
(5) After climate change in 1989–2020 there was a significant increase in ND_{FL} (even by 1 month) detected in about 2/3 of the area of Poland (in the central and western parts of the country).
(6) With the change in the NA THC phase and the macro-circulation conditions, there was also a change in the spatial distribution of areas drained by rivers with increased ND_{FL}. In 1951–1988, these included the eastern parts of Poland, while after the climate change (1989–2020)—its western and south-western parts.

Author Contributions: Conceptualization, D.W., A.A.M. and A.S.; methodology, D.W., A.A.M. and A.S.; software, D.W., A.A.M., L.S. and A.S.; validation, D.W., A.A.M. and A.S.; formal analysis, D.W., A.A.M. and A.S.; investigation and data curation, D.W., A.A.M. and A.S.; writing—original draft preparation, D.W., A.A.M., L.S. and A.S.; writing—review and editing, L.S.; visualization, D.W., A.A.M. and A.S.; supervision, D.W. and L.S. All authors have read and agreed to the published version of the manuscript.

Funding: The research was carried out under the internal research grant (internal faculty research grant) at the Faculty of Geographical and Geological Sciences of Adam Mickiewicz University in Poznań, Poland.

Institutional Review Board Statement: Not applicable.

Informed Consent Statement: Not applicable.

Data Availability Statement: The data presented in this study are available on request from the corresponding author.

Acknowledgments: We thank the editor and reviewers for their comments and suggestions, which have significantly helped us to improve the manuscript.

Conflicts of Interest: The authors declare no conflict of interest.

Appendix A

Table A1. Basic data on the studied rivers.

No.	River	Water Gauge	Longitude (°E)	Latitude (°N)	Catchment Area (km^2)	Runoff Depth [mm]	River Regime *
1	Odra	Chałupki	18.33	49.92	4666	282.4	4
2	Odra	Racibórz-Miedonia	18.23	50.12	6744	300.8	4
3	Odra	Ścinawa	16.44	51.41	29,584	188.9	4
4	Odra	Cigacice	15.61	52.03	40,106	170.6	2
5	Odra	Połęcko	14.89	52.05	47,370	167.1	2
6	Odra	Słubice	14.56	52.35	53,600	174.2	2
7	Odra	Gozdowice	14.32	52.76	109,729	146.9	2
8	Sumina	Nędza	18.31	50.16	94.4	191.3	4
9	Biała	Dobra	17.90	50.45	353	99.4	4
10	Nysa Kłodzka	Bystrzyca Kłodzka	16.65	50.29	260	466.7	4
11	Nysa Kłodzka	Kłodzko	16.66	50.44	1084	364.9	4
12	Nysa Kłodzka	Nysa	17.34	50.48	3276	278.6	4
13	Nysa Kłodzka	Skorogoszcz	17.67	50.76	4514	249.8	4
14	Bystrzyca Dusznicka	Szalejów Dolny	16.60	50.42	175	378.1	2
15	Ścinawka	Tłumaczów	16.44	50.55	256	279.8	2
16	Ścinawka	Gorzuchów	16.57	50.49	511	274.8	4
17	Biała Głuchołaska	Głuchołazy	17.38	50.32	283	542.0	4
18	Bystrzyca	Krasków	16.58	50.92	683	205.9	4
19	Piława	Mościsko	16.58	50.78	291	172.6	4
20	Strzegomka	Łażany	16.49	50.95	356	198.0	4
21	Barycz	Osetno	16.46	51.63	4579	101.6	3
22	Bóbr	Żagań	15.32	51.62	4254	275.8	4
23	Kamienica	Barcinek	15.60	50.94	97.2	389.7	2
24	Kwisa	Nowogrodziec	15.40	51.20	736	306.9	4
25	Warta	Działoszyn	18.87	51.11	4088	185.8	2
26	Warta	Sieradz	18.74	51.60	8140	171.3	2
27	Warta	Poznań	16.95	52.40	25,126	124.5	2
28	Warta	Skwierzyna	15.50	52.60	31,268	123.4	2
29	Warta	Gorzów Wielkopolski	15.25	52.73	52,186	124.4	2
30	Oleśnica	Niechmirów	18.76	51.39	592	126.7	3
31	Ner	Dąbie	18.82	52.08	1712	181.6	2
32	Prosna	Mirków	18.16	51.32	1255	126.0	2
33	Prosna	Piwonice	18.11	51.73	2938	119.2	2
34	Prosna	Bogusław	17.95	51.90	4304	114.3	2
35	Niesób	Kuźnica Skakawska	18.13	51.28	246	123.8	3
36	Ołobok	Ołobok	18.07	51.64	447	110.7	3
37	Mogilnica	Konojad	16.53	52.15	663	77.3	3
38	Wełna	Pruśce	17.10	52.77	1130	92.5	3
39	Flinta	Ryczywół	16.84	52.82	276	74.1	3
40	Sama	Szamotuły	16.58	52.61	395	83.4	3

Table A1. *Cont.*

No.	River	Water Gauge	Longitude (°E)	Latitude (°N)	Catchment Area (km^2)	Runoff Depth [mm]	River Regime *
41	Noteć	Nowe Drezdenko	15.84	52.85	15,970	143.2	2
42	Gwda	Piła	16.74	53.15	4704	180.0	1
43	Drawa	Drawsko Pomorskie	15.81	53.53	609	209.2	2
44	Ina	Goleniów	14.83	53.56	2163	185.5	2
45	Rega	Trzebiatów	15.26	54.06	2628	239.4	2
46	Parsęta	Tychówko	16.07	53.90	896	289.1	2
47	Wieprza	Stary Kraków	16.61	54.44	1519	327.0	1
48	Słupia	Słupsk	17.03	54.47	1450	338.5	1
49	Łupawa	Smołdzino	17.21	54.66	805	325.7	1
50	Wisła	Skoczów	18.79	49.80	297	641.0	4
51	Wisła	Goczałkowice	18.99	49.93	738	381.0	5
52	Wisła	Jawiszowice	19.12	49.97	971	426.1	5
53	Wisła	Bieruń Nowy	19.19	50.06	1748	381.8	4
54	Wisła	Jagodniki	20.68	50.20	12,058	334.4	4
55	Wisła	Szczucin	21.08	50.33	23,901	307.4	4
56	Wisła	Sandomierz	21.75	50.67	31,846	284.8	4
57	Wisła	Zawichost	21.86	50.81	50,732	261.9	4
58	Wisła	Annopol	21.83	50.89	51,518	261.8	4
59	Wisła	Dęblin	21.83	51.56	68,234	227.9	4
60	Wisła	Toruń	18.61	53.01	181,033	167.5	2
61	Wisła	Tczew	18.80	54.10	194,376	167.3	2
62	Soła	Oświęcim	19.22	50.04	1386	473.1	4
63	Skawa	Sucha Beskidzka	19.61	49.74	468	507.9	4
64	Skawa	Wadowice	19.51	49.88	836	465.0	4
65	Raba	Proszówki	20.43	50.00	1470	356.6	4
66	Dunajec	Krościenko	20.43	49.44	1580	634.9	5
67	Dunajec	Nowy Sącz	20.69	49.63	4341	472.8	4
68	Poprad	Muszyna	20.89	49.34	1514	365.9	4
69	Poprad	Stary Sącz	20.66	49.57	2071	380.5	4
70	Biała	Koszyce Wielkie	20.95	50.00	957	290.5	4
71	Nida	Brzegi	20.41	50.74	2259	177.1	2
72	Nida	Pińczów	20.52	50.51	3352	168.2	2
73	Czarna Nida	Tokarnia	20.45	50.77	1216	171.4	2
74	Czarna	Połaniec	21.28	50.43	1354	149.2	3
75	Wisłoka	Żółków	21.46	49.73	581	384.7	4
76	Ropa	Klęczany	21.22	49.70	483	406.9	4
77	Brzeźnica	Brzeźnica	21.49	50.11	484	212.5	4
78	Koprzywianka	Koprzywnica	21.57	50.60	502	127.1	3
79	San	Lesko	22.32	49.47	1614	555.0	4
80	San	Przemyśl	22.77	49.78	3686	444.9	4
81	San	Jarosław	22.70	50.02	7041	312.7	4
82	San	Radomyśl	21.93	50.67	16,824	241.6	4
83	Osława	Zagórz	22.27	49.51	505	509.0	4
84	Wiar	Krówniki	22.82	49.77	789	252.7	4
85	Wisznia	Nienowice	22.92	49.94	1185	178.6	4
86	Wisłok	Krosno	21.77	49.69	596	327.8	4
87	Wisłok	Żarnowa	21.82	49.88	1427	287.3	4
88	Wisłok	Rzeszów	22.02	50.04	2086	263.1	4
89	Wisłok	Tryńcza	22.55	50.16	3516	227.7	4
90	Mleczka	Gorliczyna	22.49	50.08	529	173.2	4
91	Tanew	Harasiuki	22.47	50.48	2034	189.7	2
92	Kamienna	Wąchock	21.02	51.08	476	192.7	2
93	Wieprz	Zwierzyniec	22.97	50.61	405	160.1	1
94	Wieprz	Krasnystaw	23.18	50.99	3001	129.8	2
95	Wieprz	Lubartów	22.64	51.50	6364	111.7	2
96	Wieprz	Kośmin	22.00	51.57	10,231	113.2	2

Table A1. *Cont.*

No.	River	Water Gauge	Longitude (°E)	Latitude (°N)	Catchment Area (km^2)	Runoff Depth [mm]	River Regime *
97	Bystrzyca	Sobianowice	22.69	51.30	1265	125.6	2
98	Pilica	Przedbórz	19.88	51.09	2536	185.9	2
99	Pilica	Nowe Miasto	20.57	51.61	6717	166.9	2
100	Pilica	Białobrzegi	20.95	51.66	8664	160.4	2
101	Wolbórka	Zawada	19.94	51.53	616	137.5	2
102	Drzewiczka	Odrzywół	20.56	51.52	1004	166.9	2
103	Narew	Narew	23.52	52.92	1978	146.0	3
104	Narew	Suraż	22.96	52.95	3376	139.5	3
105	Narew	Strękowa Góra	22.54	53.22	7181	141.4	3
106	Narew	Wizna	22.41	53.20	14,308	148.4	3
107	Narew	Piątnica-Łomża	22.09	53.19	15,296	150.9	3
108	Narew	Nowogród	21.86	53.23	20,106	152.4	3
109	Narew	Ostrołęka	21.56	53.08	21,862	155.8	3
110	Narewka	Narewka	23.73	52.86	590	156.9	3
111	Supraśl	Fasty	23.03	53.18	1817	153.3	2
112	Biebrza	Sztabin	23.12	53.67	846	171.5	3
113	Biebrza	Dębowo	22.93	53.61	2322	167.3	3
114	Biebrza	Osowiec	22.64	53.48	4365	160.0	3
115	Biebrza	Burzyn	22.46	53.27	6900	158.0	3
116	Brzozówka	Karpowicze	23.04	53.59	650	154.1	3
117	Pisa	Ptaki	21.79	53.39	3562	181.6	1
118	Pisa	Dobrylas	21.87	53.28	4061	182.4	2
119	Rozoga	Myszyniec	21.34	53.39	231	155.2	2
120	Omulew	Krukowo	21.11	53.31	1265	170.0	2
121	Orzyc	Krasnosielc	21.15	53.04	1268	142.2	2
122	Bug	Włodawa	23.57	51.55	14,410	120.5	3
123	Bug	Frankopol	22.56	52.41	31,336	118.1	3
124	Bug	Wyszków	21.45	52.59	39,119	122.5	3
125	Włodawka	Okuninka	23.52	51.52	576	116.5	3
126	Krzna	Malowa Góra	23.47	52.10	3128	108.1	3
127	Nurzec	Boćki	23.04	52.65	556	134.0	3
128	Nurzec	Brańsk	22.82	52.74	1227	126.8	3
129	Liwiec	Łochów	21.68	52.51	2466	134.1	3
130	Drwęca	Nowe Miasto Lubawskie	19.59	53.42	2725	188.9	2
131	Drwęca	Brodnica	19.40	53.26	3526	192.5	2
132	Drwęca	Elgiszewo	18.93	53.06	4959	173.7	2
133	Wel	Kuligi	19.69	53.43	764	206.3	1
134	Brda	Tuchola	17.90	53.57	2462	248.6	1
135	Wda	Czarna Woda	18.09	53.84	940	210.7	1
136	Wierzyca	Brody Pomorskie	18.76	53.86	1544	175.0	2
137	Łyna	Sępopol	21.01	54.27	3647	211.7	2
138	Guber	Prosna	21.09	54.23	1568	171.6	2
139	Gołdapa	Banie Mazurskie	22.03	54.25	548	266.9	3
140	Czarna Hańcza	Czerwony Folwark	23.12	54.07	454	262.6	2

Note: * Types of river regime: 1—nival poorly developed, 2—nival moderately developed, 3—nival strongly developed, 4—nival-pluvial, 5—pluvial-nival. Source: After [59,60], modified.

References

1. Schmuck, A. *Outline of Hydrometeorology*; Wydawnictwo Naukowe PWN: Wrocław-Warsaw, Poland, 1960; pp. 1–108. (In Polish)
2. Bac, S. Studies on evaporation of free water surface field, field evaporation and potential evapotranspiration. *Zesz. Nauk. WSR We Wrocławiu* **1968**, *80, Melioracja 13*, 7–68. (In Polish)
3. Kędziora, A. *Fundamentals of Agro-Meteorology*; Państwowe Wydawnictwo Rolnicze i Leśne: Warsaw, Poland, 1999; pp. 1–364. (In Polish)
4. Giuntoli, I.; Renard, B.; Vidal, J.-P.; Bard, A. Low flows in France and their relationship to large-scale climate indices. *J. Hydrol.* **2013**, *482*, 105–118. [CrossRef]

5. Shorthouse, C.; Arnell, N. Spatial and temporal variability in European river flows and the North Atlantic Oscillation. In *FRIEND 97-Regional Hydrology: Concepts and Models for Sustainable Water Resource Management*; IAHS Publ: Wallingford, UK, 1997; Volume 246.
6. Bouwer, L.M.; Vermaat, J.E.; Aerts, J.C.J.H. Regional sensitivities of mean and peak river discharge to climate variability in Europe. *J. Geophys. Res.* **2008**, *113*, D19103. [CrossRef]
7. Wilby, R.; O'Hare, G.; Barnsley, N. The North Atlantic Oscillation and British Isles climate variability, 1865–1996. *Weather* **1997**, *52*, 266–276. [CrossRef]
8. Kiely, G. Climate change in Ireland from precipitation and streamflow observations. *Adv. Water Resour.* **1999**, *23*, 141–151. [CrossRef]
9. Kingston, D.G.; Hannah, D.M.; Lawler, D.M.; McGregor, G.R. *Interactions between Large-Scale Climate and River Flow across the Northern North Atlantic Margin*; IAHS-AISH Publ: Havana, Cuba, 2006; pp. 350–355.
10. Wedgbrow, C.S.; Wilby, R.L.; Fox, H.R.; O'Hare, G. Prospects for seasonal forecasting of summer drought and low river flow anomalies in England and Wales. *Int. J. Climatol.* **2002**, *22*, 219–236. [CrossRef]
11. Stefan, S.; Ghioca, M.; Rimbu, N.; Boroneant, C. Study of meteorological and hydrological drought in southern Romania from observational data. *Int. J. Climatol.* **2004**, *24*, 871–881. [CrossRef]
12. Mager, P.; Kuźnicka, M.; Kępińska-Kasprzak, M.; Farat, R. Changes in the intensity and frequency of occurrence of droughts in Poland (1891–1995). *Geogr. Pol.* **2000**, *73*, 41–48.
13. Łabędzki, L. Estimation of local drought frequency in central Poland using the standardized precipitation index SPI. *Irrig. Drain.* **2007**, *56*, 6777. [CrossRef]
14. Tokarczyk, T. Widely applied indices for drought assessment and Polish application. In *Infrastruktura i Ekologia Terenów Wiejskich*; Stowarzyszenie Infrastruktura i Ekologia Terenów Wiejskich: Kraków, Poland, 2008; Volume 7, pp. 167–182. (In Polish)
15. Tokarczyk, T. *Low-Water Flows as an Indicator of Hydrological Drought*; Instytut Meteorologii i Gospodarki Wodnej: Warsaw, Poland, 2010; pp. 1–164. (In Polish)
16. Tokarczyk, T. Classification of low flow and hydrological drought for a river basin. *Acta Geophys.* **2013**, *61*, 404–421. [CrossRef]
17. Szalińska, W. Combined analysis of precipitation and water deficit for drought hazard assessment. *Hydrol. Sci. J.* **2014**, *59*, 1675–1689. [CrossRef]
18. Tomaszewski, E.; Kozek, M. Dynamics, Range, and Severity of Hydrological Drought in Poland. In *Management of Water Resources in Poland*; Zeleňáková, M., Kubiak-Wójcicka, K., Negm, A.M., Eds.; Springer Nature: Cham, Switzerland, 2021. [CrossRef]
19. Tomaszewski, E.; Kubiak-Wójcicka, K. 2021: Low-Flows in Polish Rivers. In *Management of Water Resources in Poland*; Zeleňáková, M., Kubiak-Wójcicka, K., Negm, A.M., Eds.; Springer Nature: Cham, Switzerland, 2021. [CrossRef]
20. Szwed, M.; Karg, G.; Pinskwar, I.; Radziejewski, M.; Graczyk, D.; Kędziora, A.; Kundzewicz, Z.W. Climate change and its effect on agriculture, water resources and human health sectors in Poland. *Nat. Hazards Earth Syst. Sci.* **2010**, *10*, 1725–1737. [CrossRef]
21. Meresa, H.K.; Osuch, M.; Romanowicz, R. Hydro-Meteorological Drought Projections into the 21-st Century for Selected Polish Catchments. *Water* **2016**, *8*, 206. [CrossRef]
22. Instytut Meteorologii i Gospodarki Wodnej–Państwowy Instytut Badawczy. Dane Publiczne. Available online: https://danepubliczne.imgw.pl (accessed on 20 May 2021). (In Polish)
23. Bryś, K. *Dynamics of Net Radiation Balance of Grass Surface and Bare Soil*; Monografie CLXII, Wydawnictwo Uniwersytetu Przyrodniczego we Wrocławiu: Wrocław, Poland, 2013; pp. 1–288. (In Polish)
24. Matuszko, D. Long-term variability in solar radiation in Krakow based on measurements of sunshine duration. *Int. J. Climatol.* **2014**, *34*, 228–234. [CrossRef]
25. Matuszko, D.; Piotrowicz, K. Relationship between sunshine duration and air temperature on the basis of long-term climatological series in Krakow (1884–2016). *Przegląd Geofiz.* **2018**, *63*, 15–29. (In Polish)
26. Podstawczyńska, A. The solar characteristics of climate of Łódź. *Acta Univ. Lodz. Folia Geogr. Phys.* **2007**, *7*, 1–220. (In Polish)
27. Dimitriev, A.A.; Dubravin, V.F.; Belyazo, V.A. *The Atmospheric Processes in the Northern Hemisphere (1891–2018), Their Classification and Use*; SUPER Izdatielstvo: Sankt Petersburg, Russia, 2018; pp. 1–305. (In Russian)
28. Kalnay, E.; Kanamitsu, M.; Kistler, R.; Collins, W.; Deaven, D.; Gandin, L.; Iredell, M.; Saha, S.; White, G.; Woollen, J.; et al. The NCEP/NCAR 40-Year Reanalysis Project. *Bull. Am. Meteorol. Soc.* **1996**, *77*, 437–471. [CrossRef]
29. Okołowicz, W. *General Climatology*; Wydawnictwo Naukowe PWN: Warsaw, Poland, 1976; pp. 1–422. (In Polish)
30. Kędziora, A. Water balance of Konin strip mine landscape in changing climatic conditions. *Rocz. Glebozn.* **2008**, *59*, 104–118. (In Polish)
31. Radzka, E. Climatic water balance for the vegetation season (according to Ivanov's equation) in Central-Eastern Poland. *Woda-Środowisko-Obsz. Wiej.* **2014**, *14*, 67–76. (In Polish)
32. Okoniewska, M.; Szumińska, D. Changes in Potential Evaporation in the Years 1952–2018 in North-Western Poland in Termsof the Impact of Climatic Changes on Hydrological an Hydrochemical Condotions. *Water* **2020**, *12*, 877. [CrossRef]
33. Yevjevich, V. *An Objective Approach to Definitions and Investigations of Continental Hydrologic Droughts. Hydrology Papers*; Colorado State University: Fort Collins, CO, USA, 1967; pp. 1–25.
34. Ozga-Zielińska, M.; Brzeziński, J. *Applied Hydrology*; Wydawnictwo Naukowe PWN: Warsaw, Poland, 1994; pp. 1–323. (In Polish)
35. Wangengejm, G.Y. Fundamentals of macrocirculation method for long-range weather forecasting for the Arctic. In *Trudy*; AANII: Leningrad, USSR, 1952; Volume 34, pp. 1–314. (In Russian)

36. Girs, A.A. On the creation of a single classification of the northern hemisphere. *Meteorol. I Gidrol.* **1964**, *4*, 43–47. (In Russian)
37. Girs, A.A. *Long-Term Atmospheric Circulation Variations, and Long-Range Hydrometeorological Forecasts*; Girometeoizdat: Leningrad, USSR, 1971; pp. 1–280. (In Russian)
38. Savichev, A.I.; Mironicheva, N.P.; Cepelev, V.Y. Atmospheric circulation characteristics of the northern hemisphere of the Atlantic-Eurasian sector for last decades. *Uchenye Zap. Ross. Gos. Gidrometeorol. Univ.* **2015**, *39*, 120–131. (In Russian)
39. Degirmendžić, J.; Kożuchowski, K. Circulation epochs based on the Vangengeim-Girs large scale patterns (1891–2010). *Acta Univ. Lodz. Folia Geogr. Phys.* **2018**, *17*, 7–13. [CrossRef]
40. Degirmnedžić, J.; Kożuchowski, K. Variation of macro-circulation forms over the Atlantic-Eurasian temperate zone according to the Vangengeim-Girs classification. *Int. J. Climatol.* **2019**, *39*, 4938–4942. [CrossRef]
41. Monin, A.S. *An Introduction to the Theory of Climate*; Gidrometoizdat: Leningrad, USSR, 1982; pp. 1–246. (In Russian)
42. Marsz, A.A.; Styszyńska, A. The Influence of the Sign of NAO Phases during the Winter Period on the Water Balance and the Possibility of Drought Occurrence in the Warm Season in Poland. *Ann. Univ. Mariae Curie-Skłodowska* **2021**, *76*, 127–143. [CrossRef]
43. Hill, T.; Lewicki, P. *Statistics: Methods and Applications*; StatSoft: Tulsa, OK, USA, 2007.
44. Bednorz, E. Snow cover in eastern Europe in relation to temperature, precipitation and circulation. *Int. J. Climatol.* **2004**, *24*, 591–601. [CrossRef]
45. Czarnecka, M. Frequency of occurrence and depth of snow cover in Poland. *Acta Agrophys.* **2012**, *19*, 501–514. (In Polish)
46. Tomczyk, A.M. Impact of macro-scale circulation types on the occurrence of snow cover in Europe. *Acta Geogr. Sil.* **2014**, *15*, 65–69. (In Polish)
47. Pociask-Karteczka, J. River Hydrology and the North Atlantic Oscillation: A General Review. *AMBIO* **2006**, *35*, 312–314. [CrossRef] [PubMed]
48. Styszyńska, A.; Tamulewicz, J. Warta river discharges in Poznań and atmospheric circulation in the North Atlantic region. *Quaest. Geogr.* **2004**, *23*, 63–81.
49. Wrzesiński, D. Changes of the hydrological regime of rivers of northern and central Europe in various circulation periods of the North Atlantic Oscillation. *Quaest. Geogr.* **2005**, *24*, 97–109.
50. Wrzesiński, D. Typology of spatial patterns seasonality in European rivers flow regime. *Quaest. Geogr.* **2008**, *27*, 87–98.
51. Wrzesiński, D. Regional differences in the influence of the North Atlantic Oscillation on seasonal river runoff in Poland. *Quaest. Geogr.* **2011**, *30*, 127–136. [CrossRef]
52. Wrzesiński, D.; Paluszkiewicz, R. Spatial differences in the impact of the North Atlantic Oscillation on the flow of rivers in Europe. *Hydrol. Res.* **2011**, *42*, 30–39. [CrossRef]
53. Marsz, A.A.; Styszyńska, A. Intensity of thermohaline Circulation in the North Atlantic and Droughts in Poland. *Pr. I Studia Geogr.* **2021**, *66*, 63–88. (In Polish) [CrossRef]
54. Marsz, A.A.; Styszyńska, A.; Krawczyk, W.E. Long-term fluctuations of annual discharges of the main rivers in Poland and their association with the Northern Atlantic Thermohaline Circulation. *Przegląd Geogr.* **2016**, *88*, 295–316. (In Polish) [CrossRef]
55. Wrzesiński, D.; Marsz, A.A.; Styszyńska, A.; Sobkowiak, L. Effect of the North Atlantic Thermohaline Circulation on Changes in Climatic Conditions and River Flow in Poland. *Water* **2019**, *11*, 1662. [CrossRef]
56. Fortak, H. *Meteorology*; Deutsche Buch-Gemainschaft: Berlin, Germany; Darmstadt, Germany; Wien, Austria, 1971; pp. 1–287. (In German)
57. Zvieriev, A.S. *Synoptic Meteorology*; Gidrometeoizdat: Leningrad, USSR, 1977; pp. 1–711. (In Russian)
58. Stachý, J. Long-term forecast of the runoff of Polish rivers. In *PIH-M Wiadomości Służby Hydrol. i Meteorol*; Państwowy Instytut Hydrologiczno-Meteorologiczny: Warsaw, Poland, 1969; Volume 3, pp. 23–34. (In Polish)
59. Wrzesiński, D. Use of Entropy in the Assessment of Uncertainty of River Runoff Regime in Poland. *Acta Geophys.* **2016**, *64*, 1825–1839. [CrossRef]
60. Wrzesiński, D. Flow Regime Patterns and Their Changes. In *Management of Water Resources in Poland*; Zeleňáková, M., Kubiak-Wójcicka, K., Negm, A.M., Eds.; Springer Nature: Cham, Switzerland, 2021; pp. 163–180. [CrossRef]